Post-Earthquake Bridge Repair Cost Evaluation Methodology

Kevin Mackie, John-Michael Wong, and Bozidar Stojadinovic

ABSTRACT

Post-earthquake repair costs are important for evaluating the performance of new bridge design options and different existing bridge configurations in the next major earthquake. Hazard and structural demand models provide information on the probabilistic structural response during earthquakes. Damage and decision models are needed to link the structural response to decisions on bridge repair actions and repair costs. A new step-by-step probabilistic repair cost methodology is proposed in this paper to evaluate the costs of repairs for different bridge components and the bridge as a system corresponding to varying degrees of damage. Repair actions, quantities, and costs are input into spreadsheet templates and a numerical tool evaluates expected repair costs and repair cost variance for a range of earthquake intensities. Central to the proposed methodology is the concept of performance groups—groups defined to account for bridge components that are repaired together. Six spreadsheets are used to track all of the necessary data: bridge information, structural response, component damage states, repair methods and repair quantities, and unit costs or production rates. Data can be customized for repair methods and bridge types particular to different state departments of transportation. The methodology is illustrated using repair cost fragilities for a typical multi-span reinforced concrete highway overpass bridge in California.

Kevin Mackie, Assistant Professor, Dept. of Civil & Env., Engineering, University of Central Florida, Orlando, FL 32816-2450

John-Michael Wong, Graduate Student, Dept. of Civil & Env., Engineering, 721 Davis Hall #1710, University of California, Berkeley, CA 94720-1710

Bozidar Stojadinovic, Associate Professor, Dept. of Civil & Env., Engineering, 721 Davis Hall #1710, University of California, Berkeley, CA 94720-1710

INTRODUCTION

A large portion of bridges in the current California bridge inventory share similar construction characteristics, especially those owned and maintained by the California Department of Transportation (Caltrans). Probabilistic evaluation of the performance of these bridges under rare, but strong, ground motions is therefore essential for successful evaluation of the entire regional transportation network performance during and after an earthquake. Additionally, probabilistic quantification of bridge seismic performance and vulnerability provides insight into the shortcomings of current designs and into the potential advantages of proposed new technologies at varying levels of seismic hazard and for different site conditions. Performance of bridges at the demand, damage, and loss levels can be evaluated using the Pacific Earthquake Engineering Research (PEER) Center's probabilistic performance-based seismic evaluation framework. Of particular interest in this paper is developing probabilities of exceeding different levels of repair costs, rather than focusing strictly on engineering quantities.

One implementation of the PEER framework (Cornell and Krawinkler, 2000) is presented for evaluating a typical benchmark reinforced concrete bridge typical of new construction in California. Models of these structures are created that account for the nonlinear behavior of the columns, deck, abutments, and expansion joints at the abutments. Seismic demand models are then developed using nonlinear time history analysis, considering both near- and far-field excitation types. Damage in the bridge components is determined using experimental and empirical databases. Structural components are then classified into performance groups according to the repair methods corresponding to their damage states. Finally, approximate repair cost ratios are estimated from the assembly of discrete damage states from all performance groups.

A rigorous yet practical implementation of a performance-based earthquake engineering methodology is developed and demonstrated for the example bridge. To define performance objectives, performance quantities are defined by the probability of exceeding threshold values of socio-economic decision variables (DVs) in the seismic hazard environment under consideration—in this case repair cost ratios. The PEER PBEE framework utilizes the total probability theorem to disaggregate the problem into several intermediate probabilistic models that address sources of randomness and uncertainty more objectively. This disaggregation of the decision-making framework involves the following intermediate variables: repair quantities (Q), damage measures (DMs), engineering demand parameters (EDPs), and seismic hazard intensity measures (IMs). Effective aggregation of decision data requires associating structural elements and assemblies into performance groups (PGs) using the correlations imposed by the commonly used repair methods.

These PGs and associated data are tracked using a spreadsheet implementation of a database in this paper. The methodology for associating these spreadsheets with the components of the PEER framework is demonstrated in this paper. Particularly, the loss model that relates measures of damage (DM) to repair quantities (Q) is reformulated to more accurately capture the response of the testbed bridge as calibrated using realistic damage and loss scenarios (Wong et al., 2008). Previous implementations of the PEER framework (Mackie et al., 2006; Mackie et al., 2007) were based on the power-law relationship between DM and Q (or DV):

$$\ln Q = E + F \ln(DM) \tag{1}$$

METHODOLOGY

For each structural component of the bridge (or performance group) and repair quantity, a single scalar-type analysis is performed, modeled in IM-EDP-DM-Q space. When solved using the closed-form or Fourway solution strategies, the expectation and variance of each repair quantity $q_{n,l}$ for the repair item n and performance group l are obtained. The first moment and second central moment are denoted E[$q_{n,l}$] and Var[$q_{n,l}$], respectively. These two quantities are lognormal distribution parameters due to the assumptions surrounding the Fourway process (technically, the second lognormal parameter is the square root of the variance).

Because the repair quantity loss model cannot be assumed to be a power-law relationship, a different median relationship between Q and DM must be derived. A power-law relationship would grow exponentially beyond the data provided, and would not accurately define distinct plateaus of repair data. Choosing instead to use a log-linear relationship between discrete repair quantities is an intuitive choice because earthquake damage and the resulting repair methods and quantities are, by nature, continuous processes that are not completely defined by the discrete damage states and repair quantities for which data exist. So, the general form of the Q-DM model used is a piecewise linear relationship in log space. Two additional considerations are necessary for formulating the Q-DM relationship. First, the repair quantities are not necessarily increasing with greater damage. For example, from low to moderate damage, the amount of patching for concrete cover spalling on a column increases. However, beyond a certain damage measure value, the amount of patching drops to zero because the preferred repair method becomes complete replacement instead of rehabilitation. This necessitates the use of a curtailed Q-DM relationship for certain items. By curtailing a repair quantity loss model, it may be possible for the overall repair cost to be discontinuous (a decrease) with increasing IM. Second, because no simulations are performed in this method, the outcome is dependent on the ability to discern first and second moments of Q. This prevents the use of zero- or large-slope Q-DM models because the variance is dependent on these slopes.

Previous attempts (Mackie et al., 2006; Mackie et al., 2007) to address these two considerations utilized four general categories of typical Q-DM model behavior. The previous procedure was tailored to suit the bridge data available at the time; however was prone to unpredictable behavior at demands beyond the last damage state and was difficult to extend the approach to user-specified Q-DM models without recognition of new piecewise types. The previous approach also often resulted in extremely large (and unlikely) values of dispersion for the repair quantities when there are large jumps in the quantity magnitudes between damage states, and occasionally led to discontinuities in the median Q-DM relationship when trying to best fit linear curves in log space to the data points. Nevertheless, the benefit of using the previous approach was a closed-form solution strategy was easily applied to each piecewise linear (in log space) portion of the Q-DM model.

Therefore, a new approach was developed that overcomes all of the issues experienced by the previous approach, plus it retains the simplicity of automated closed-form solutions. The new approach is based on linearization of the Q-DM model (linear in linear space). Rather than assuming that the loss model follows a power-law relationship, a loss model that is linear in linear space can be written as Eq. 2. The first-order expansion of ln(Q) in Eq. 2 about a point in DM space denoted d_0 can be written as Eq. 3.

$$Q = e_{lin} DM + f_{lin} \tag{2}$$

$$\ln(Q) = \ln\left(e_{lin}d_0 + f_{lin}\right) + \frac{e_{lin}}{e_{lin}d_0 + f_{lin}}\left(DM - d_0\right) + h.o.t. \tag{3}$$

Similarly DM and d_0 can be related to ln(DM) and ln(d_0) and combined with Eq. 3 to obtain the same form as Eq. 1, but with new parameters E' (Eq. 4) and F' (Eq. 5) replacing the previous parameters E and F.

$$E' = \ln\left(e_{lin}d_0 + f_{lin}\right) - \frac{e_{lin}d_0 \ln\left(d_0\right)}{e_{lin}d_0 + f_{lin}} \tag{4}$$

$$F' = \frac{e_{lin}d_0}{e_{lin}d_0 + f_{lin}} \tag{5}$$

While easy to implement, the new parameters still require selection of an expansion point d_0 and do not guarantee that the denominator does not equal zero or that the resulting piecewise Q-DM function is continuous at the end-points of the intervals used. The new procedure is complete as implemented in this paper by continuously updating the location of the linearization point d_0 to be at every DM input desired. This results in well-behaved Q-DM models that are in fact linear in linear space but are compatible with the previous closed-form solution strategy.

A final improvement that is implemented is the concept of DS0 and DS∞. The DS0 damage state corresponds to the onset of damage when repair costs begin to accumulate. For analysis, the repair cost of the bridge is treated as $0 below the DS0 level of damage. Damage beyond DS0 is where repairs are needed and costs begin to accumulate. Even though the defined damage states are discrete, the moment-based computation method assumes that a continuous range of damage exists between the discrete states. This assumption allows for the closed-form computation of the PEER integral using the Fourway method. This computation method requires the definition of maximum possible repair quantities to define an upper limit to the quantities and costs. The upper limit is called DS∞, since it corresponds to the most severe possible damage state for the elements in a performance group. DS∞ usually corresponds to complete failure and replacement of all the elements in the entire performance group.

Once the quantities for individual repair items and performance groups are determined, the total quantity of the same repair item across all performance groups can be computed. A total number of N_{PG} performance groups and N_Q repair items were used. The expected value and variance of each of the repair quantities was then computed, rather than the complete probability distribution for each repair quantity. The expectation of the total repair quantity Q_n for each item n remains a linear combination of the expected performance group-dependent quantities (Eq. 6). The corresponding variances are not simple linear combinations due to the correlation between response quantities and performance groups. For a summation of correlated random variables, the variance is given as Eq. 7. The covariance is obtained from the correlation coefficient relating performance groups l and p from the nonlinear bridge analysis results.

$$E\left[Q_n\right] = \sum_{l=1}^{N_{PG}} E\left[q_{n,l}\right] \tag{6}$$

$$Var\left[Q_n\right] = \sum_{l=1}^{N_{PG}} Var\left[q_{n,l}\right] + 2\sum_{l=1}^{N_{PG}}\sum_{p>l}^{N_{PG}} Cov\left[q_{n,l}, q_{n,p}\right] \tag{7}$$

The simple summation of Q_n between performance groups is possible only if the quantities are assumed to be (or converted to) normal distributions. The unit cost Cu_n of each item n was considered to be constant regardless of the quantity Q_n. Costs associated with mobilization and contingencies can be estimated later as lump sum percentages of the total cost. The resolution of the cost data at present does not lend itself to developing a nonlinear unit cost function; however, this addition will be pursued in future studies. The total cost for each repair item is obtained by multiplying the unit cost by the repair quantity. Similarly, the variance of the cost is also dependent on $E[Q_n]$ and $Var[Q_n]$. The total expected cost of repair $E[TC]$ was then determined from:

$$E[TC] = \sum_{n=1}^{N_Q} Cu_n \left(E[Q_n] \right) \quad (8)$$

The total cost variance was obtained by summation of the individual material variances and adding an additional term due to the uncertainty in the unit cost. Because the repair items were assumed to be statistically independent, the covariance term, similar to that in Eq. 7, is zero. Based on the central limit theorem, it is likely that the total cost will approach a normal distribution due to the number of Qs being summed (N_Q Qs varied within N_{PG} PGs). The process described is easily automated by computer.

TESTBED BRIDGE

The testbed bridge is from a series of bridge types presented in the PEER lifelines project report by Ketchum et al. (2004). Of the prevalent bridge designs in the California bridge inventory, post-tensioned concrete box girder and pre-tensioned, pre-cast concrete I-girder bridges are identified as the most common. From the matrix of 11 common bridge configurations (types) developed in Ketchum et al. (2004), the straight, cast-in-place box girder bridges with five spans were selected for further study by the PEER testbed teams. Specifically, the two configurations with common deck sections and single column bents were selected for this study. The two configurations are designated as Type 1 and Type 11. Each of these two bridge types has 12 different design realizations based on different column and foundation dimensions. The designs span a range of common column dimensions that were then evaluated for a corresponding maximum seismic intensity resistance level. The bridges have 3 internal spans of 150' and 2 external spans of 120' with a total length of 690'. The bridges are cast-in-place, pre-stressed (CIP/PS) 2-cell box girder bridges with the superstructure supported on neoprene bearing pads under each of the three box webs. The only difference is the clear column heights; the Type 1 has 22' columns and the Type 11 has 50' columns. This paper focuses solely on Type 1A. This particular bridge design option has 4' diameter circular columns.

The testbed bridge is broken down into performance groups (PGs) for each major bridge superstructure, substructure, and foundation component. Each performance group represents a collection of structural components that act as a global-level indicator of structural performance and that contribute significantly to repair-level decisions. Performance groups are not necessarily the same as load-resisting structural components. For example, non-structural components may also form a performance group, since they also suffer damage and contribute to repair costs. The notion of a performance group also allows grouping several components together for related repair work.

For example, it is difficult to separate all of the individual structural components that comprise a seat-type abutment (shear key, back wall, bearings, approach slab, etc.) as they all interact during seismic excitation and their associated repair methods are coupled. Therefore, the "abutment" repair group incorporates the fact that repairs to the back wall require excavation of the approach slab.

Performance groups also address the issue of potentially double counting related repair items. Some repair items require the same preparation work such as soil excavation. For example, both back wall repair and enlargement of an abutment foundation require at least 4 ft of excavation behind the back wall. If these repair items were in different performance groups, then double counting the excavation would be a problem. But, since these repairs are inside a single performance group, the repair quantities can be defined without overlap. Bundling these related repair methods within a performance group allows for independent consideration of each performance group. The correlation between repair items from the performance groups can be handled at the demand model level in the PEER methodology, as shown in the methodology section.

The performance groups (total of 27) considered for the testbed bridge are: columns based on maximum displacement (1 PG per column), columns based on residual displacement (1 PG per column), deck/superstructure (1 PG per bridge span), abutment (1 PG per abutment), bearings (1 PG per abutment including all bearings), shear keys (1 PG per abutment including both external shear keys), approach (1 PG per approach), abutment piles (1 PG per abutment), and pile groups (1 PG per column). Further details regarding the testbed bridge and the analytical model that was developed for simulation are contained in Mackie et al. (2008).

DATA STRUCTURE AND SPREADSHEET IMPLEMENTATION

The database for the performance-based assessment of bridges is implemented using a series of Excel spreadsheets. Excel sheets were chosen for their portability and ease of editing. Spreadsheets also make it easy to capture the dependencies between pieces of information through the use of cell references. For example, volumes can be automatically recomputed if values for length dimensions are changed. Another advantage of spreadsheets is the ability to display the data in a manner that summarizes a lot of data on a single page. The spreadsheets can be thought of as different views of an underlying data model. Thinking of the data model in terms of tables shows the relationships between the spreadsheets in an explicit manner. Separate spreadsheets were generated for unit costs for each Q (Cost.xls), damage limit states for each performance group EDP (Damage.xls), EDP results from structural analysis at various IMs (EDP.xls), bridge information, dimensions, quantities for estimation (Info.xls), and repair quantities Q for each damage state and performance group (Repair.xls).

The example of a column performance group based on the maximum drift EDP will be used to demonstrate the spreadsheet data needed to support the methodology. See the paper on damage scenarios for more detail regarding the data contained in the spreadsheets (Wong et al., 2008). The EDP.xls spreadsheet contains a single line of data for each ground motion considered, but includes the EDP realizations for all PGs. The Damage.xls spreadsheet contains the median and logarithmic standard deviation that both define the fragility of the PGs for each damage state, conditioned on the selected EDP. The Repair.xls spreadsheet contains an entry for every repair quantity engaged for each possible damage state, for each performance group. Finally, the Cost.xls spreadsheet contains unit costs that are used to generate total repair costs once repair quantities have been summed between all damage states and PGs as per the methodology.

For the maximum column drift PG, four damage states are defined for each column in terms of maximum tangential column drift ratio. A total of four discrete damage states are defined for each column PG: initial cracking, concrete cover spalling, longitudinal reinforcing bar buckling, and complete failure. The median and logarithmic standard deviation that define the damage fragilities for each DS were obtained from predictive relationships obtained from a database of experimental column tests (Berry and Eberhard, 2003; Mackie and Stojadinovic, 2007). As mentioned previously, damage less than DS0 (initial cracking) is assumed negligible and not in need of repair. For DS1 with the onset of spalling, the amount of cracks to repair is estimated at 2 times the height of the column. The volume of concrete to be removed and patched is obtained from the cover depth plus 1" additional depth times 10% of the column height. DS2 is more severe and requires 4 times the height for crack repair and 25% of the height for removing and patching concrete. For DS3, the repair action is column replacement. Since the entire column is replaced, there are no concrete or steel patch repairs for this damage state. To replace the column, temporary superstructure support needs to be provided. The amount of temporary support is estimated based on the deck area requiring support. Access requires excavation and backfill of a 4' concentric circle 3' deep around the column.

Repair Cost Ratio

Normalized costs of repair are obtained by using the repair cost ratio (RCR) between the cost of repair and the cost of original new construction. This ratio is useful for comparing the performance of different bridge design options for new construction. For the evaluation of existing structures, the RCR including demolition costs might be more useful. Constructing a new bridge on the same site after an earthquake would require both demolition of the damaged bridge and construction of its replacement. The cost of new construction can be obtained using different methods. Ketchum et al. (2004) computed construction costs based on quantity estimates for each of the testbed bridge models. Also, Caltrans bridge cost estimates for planning purposes are based on the deck and type of construction. These estimates provide a range of cost/SF of deck area. The cost of new construction was adjusted by the price index to make comparisons between current 2007 cost data and the new construction costs reported in Ketchum et al. (2004) that were based on 2003 cost estimates. The unit costs for the individual repair items (Cu_n) used in this paper study are given in Mackie et al. (2008). Most unit costs are insensitive to the quantity. However, some of the repair items have higher unit costs with small quantities and lower unit costs with larger quantities. Unit cost uncertainty can be computed from the available data on previous bridge contracts. Or, a simple lump sum contingency estimate can be used to display the magnitude of total repair cost uncertainty due to possible fluctuations in unit cost.

RESULTS

An immediate benefit of this methodology is the ability to assess the intensity-dependent variation in repair cost ratios. Both the first and second probabilistic moments of repair cost ratio are calculated for each intensity level, and are shown in Figure 1 for three scenarios. It was assumed that after the summing of all of the costs from each repair quantity, the final RCR model followed a normal distribution. The first scenario, labeled "Fixed mean" and "Fixed $\pm1\sigma$" shows the loss model generated using the methodology in this paper (RCR versus IM) for testbed bridge Type 1A using the SpringAbutment module and fixed foundations. For comparison, the same model is analyzed;

however, some flexibility is introduced at the base of the columns (in the analytical model). This scenario is labeled as "Springs mean" and "Springs ±1σ." Finally, the previous results generated (Mackie et al., 2006) for the fixed column base case are included for comparison and labeled "Fourway mean" and "Fourway ±1σ."

Several important observations can be drawn from Figure 1. The repair cost ratios are intensity dependent and in this case a structure-independent IM was selected (*PGV*). This allows direct comparison between all three scenarios shown in the plot by simply selecting a target hazard level on the horizontal axis. Note that while the same structure is employed in all three scenarios, the fundamental periods are different based on modeling assumptions. In addition, while the previous approach (Fourway) and proposed approach exhibit similar overall results, the new methodology provides a higher fidelity on not only the intensity-dependent mean, but also the intensity-dependent uncertainty. Of particular note is the inclusion of DS0 that allows zero (or small) repair cost ratios for small earthquake events, but a rapid growth in the RCR after triggering of damage, whereas previous results show (unrealistically) an immediate accumulation of RCR. Finally, by introducing some flexibility into the foundation model, some of the non-column damage states are triggered at smaller intensities, leading to higher initial RCRs. However, due to the well-behaved Q-DM models (that include plateaus, for example) using the new method, both variants of the same structural model eventually converge to exactly the same RCR.

As is commonly done in seismic risk assessment, it is of interest to plot the repair cost ratio fragility curves for several different discrete hazard levels. For example, for a site in Berkeley, California, the 2%-, 10%-, and 50%-probabilities of exceeding a certain *PGA* value in 50 years were determined from USGS hazard maps. These *PGA* values were converted to *PGV* values using the firm ground conversion of 48 in./sec/g. The resulting *PGV* values are 149, 89, and 51 cm/s, respectively. The probabilistic moments at each intensity from Figure 1 were determined for each of the three hazard scenarios and plotted as complete CDFs in Figure 2. The individual curves are labeled as CDFs rather than RCR fragilities because they do not show the probability of a single loss limit state at different earthquake intensity levels.

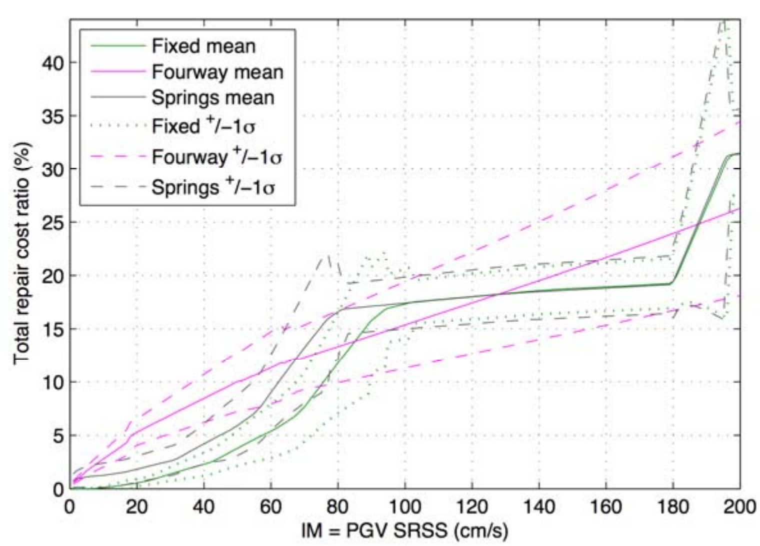

Figure 1. Repair cost ratio loss model as a function of intensity

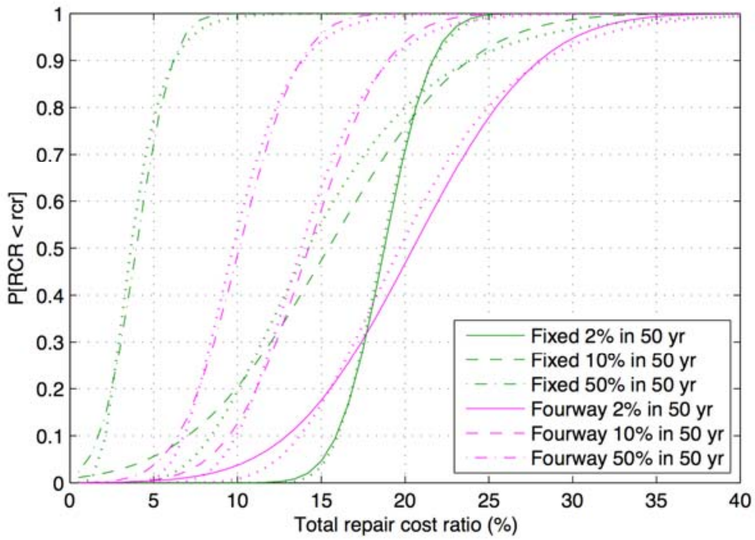

Figure 2. Repair cost ratio CDF for three hazard intensity level

Rather than generating CDFs for discrete hazard levels, it is also possible to generate standard loss fragility curves that illustrate P[RCR > *rcr* | IM = *im*]. As in Figure 2, the curves can be computed assuming that the repair cost probability distribution is normal. However, the major difference is that both the mean and standard deviation for each data point on the fragility curves is intensity dependent. Therefore, for the range of intensities where the repair cost ratios remain essentially constant, so does the probability of exceeding that RCR. The resulting fragility curves are therefore stepwise CDFs and do not necessarily appear like the CDF of a normal distribution. The fragility curves can be smoothed, for example, using a moving average window.

Disaggregation by Repair Quantity

Due to the assembly-based (vector) nature of the methodology, it is also possible to disaggregate the final repair costs into individual contributions from each repair quantity. Retaining an intensity-dependent format similar to Figure 1, the total expected cost from each repair quantity (Q) is shown in Figure 3. The ordinate is plotted in units of cost (not normalized as a RCR), and shows only the expected (mean) cost. The peak contribution at the range of intensities between 2%- and 50%- (in-50-years) exceedance probabilities is from temporary support at the abutments. However, this repair quantity is not the chief contributor at all intensities. For example, for *PGV* less than 50 cm/s, it is a low-level damage repair item (epoxy inject cracks) that controls. Conversely, at *PGV* of approximately 175 cm/s, serious damage leads to the need to replace a column and hence temporary support of the superstructure begins to rise rapidly as a contributing cost.

A similar presentation of the disaggregation of expected repair cost by repair quantity can be made by selecting discrete hazard levels of interest and plotting repair quantity contributions in the form of a pie chart. The disaggregation of expected costs at two hazard levels (2%- and 86%-in-50-years exceedance probabilities) is shown in Figure 4. The relative contribution of, for example, epoxy injecting cracks at the 86% probability of exceedance in 50 years is evident, whereas, the largest contribution is from abutment temporary support for the 2%-in-50-years hazard level.

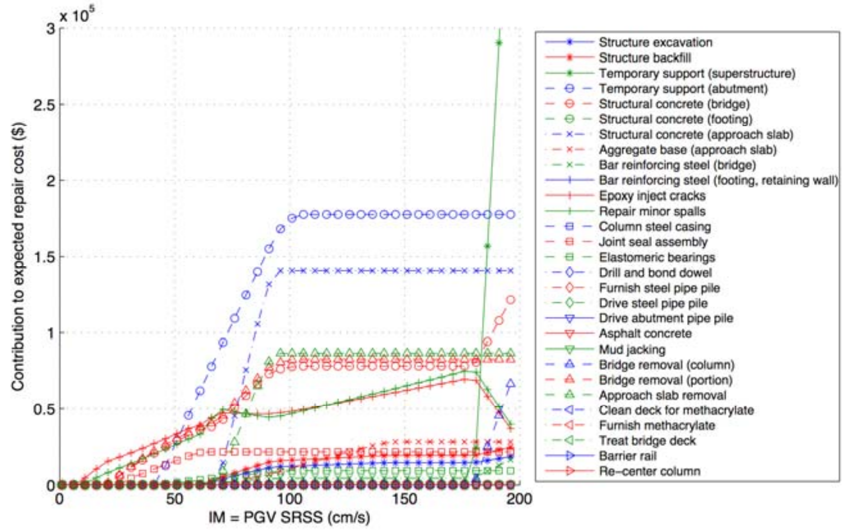

Figure 3. Disaggregation of expected repair cost by repair quantity as a function of intensity

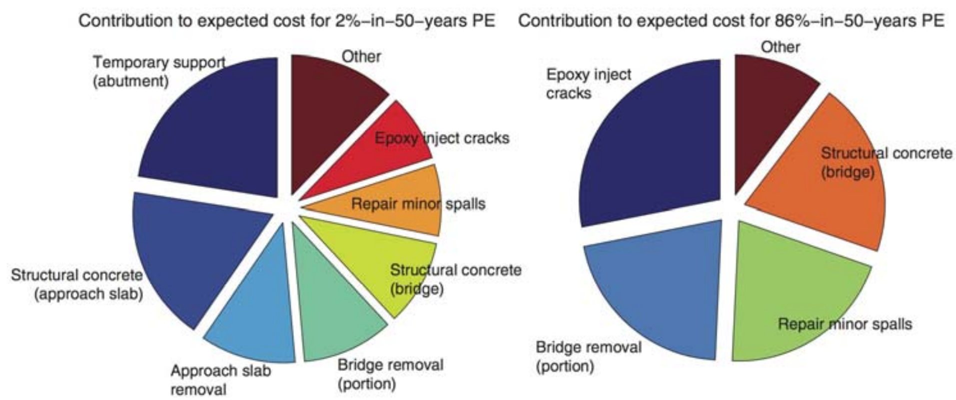

Figure 4. Disaggregation of repair cost by repair quantity for 4 discrete hazard levels

Disaggregation by Performance Group

While disaggregation by repair quantity is helpful, it does not describe specifically what component or performance group contributes most to the ultimate repair cost. It is also possible for one repair quantity to dominate because several performance groups require that item in the associated repair methods for that group. Therefore, the total expected cost was also disaggregated by performance group, as shown in Figure 5. This disaggregation is possible for the expected cost; however, it is not as straightforward to obtain the contribution of each performance group to the repair cost standard deviation due to the correlations introduced between performance groups (Eq. 7). Figure 5 provides more insight into why a repair quantity employed in several performance group repair methods features in the expected cost.

For example, bridge structural concrete contributes to a significant portion of the overall expected cost at all intensities in Figure 3. The reason for this is more readily apparent in Figure 5 as both the abutment PGs, with damage states defined in terms of the maximum longitudinal relative deck-end/abutment displacement EDPs, have the largest contribution in the range of intensities between 2%- and 50%- (in-50-years) exceedance probabilities. This indicates that the concrete is necessary to repair the back wall. The overall repair to the abutment PGs are more costly than the bearing repairs that require temporary abutment support, as would be surmised from looking at Figure 3 alone. Another illustration of information gained from Figure 5 is the sharp increase in costs at an intensity of approximately 175 cm/s. Figure 3 indicates only that this is due to the need for temporary support of the superstructure. However, from Figure 5, one is able to discern that the increase is due to the excessive maximum tangential drift ratios of columns 2 and 3 requiring support to replace the column.

CONCLUSION

Probabilistic repair cost models that are functions of earthquake intensity can be derived using the improved probabilistic moment-based approach presented in this paper. The distribution of repair costs is quantified by the expected repair cost value and variance. These two measures are obtained via interim models that disaggregate repair costs by linking individual unit costs of repair quantities, to amounts of repair materials, to damage states requiring repair, to structural response under excitation that causes damage, and finally to measures of the earthquake intensity. The interim models are tracked by a spreadsheet database implementation. The improved methodology in this paper is based on a linearization of the loss model between repair quantities and damage states. The model is linearized at each level of demand, allowing for seamless integration into previous closed-form and approximate solution strategies used in predicting post-earthquake repair costs. A major benefit of this implementation is that end-users can simply enter bridge- and state-specific repair methods and quantities into a similar database format, and the methodology does not require modification or specific case studies to remain consistent.

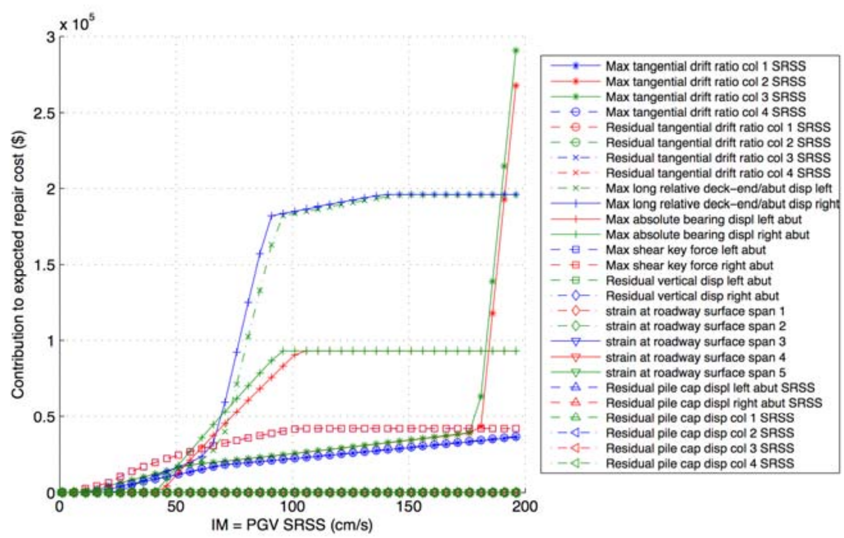

Figure 5. Disaggregation of repair cost by performance groups as a function of intensity

The proposed method is illustrated using a detailed example of a typical 5-span reinforced concrete highway bridge in California. Specific demand, damage, repair quantity, and cost models are developed for the given bridge, details of which are contained in a tandem paper (Wong et al., 2008). The response of and damage to the columns, deck, abutments, and expansion joints are taken into account. Results show how both expected repair costs and the variance of repair costs vary with intensity. Not only are the total repair costs intensity-dependent, but also the disaggregation of total repair costs by both repair quantity and performance group. This breakdown provides a higher level of information regarding damage and failure of specific bridge components or performance groups; therefore allowing better decision making regarding design or retrofit. When applied to alternate bridge configurations, the cumulative distribution functions of repair cost can be used to differentiate between different design choices in a pre-earthquake planning or design scenario. Additionally, the repair cost information can be used for classes of bridges in network simulations to estimate economic losses due to virtual earthquake events, or to better evaluate the repairs necessary on a bridge inventory after a known event.

ACKNOWLEDGMENT

This work was supported in part by the Earthquake Engineering Research Centers Program of the National Science Foundation under award number EEC-9701568 through the Pacific Earthquake Engineering Research Center. Any opinions, findings, conclusions or recommendations expressed in this material are those of the authors and do not necessarily reflect those of the National Science Foundation.

REFERENCES

Berry, M.P., and Eberhard, M.O., (2003), "Performance Models for Flexural Damage in Reinforced Concrete Columns," Report No. 2003/18, Pacific Earthquake Engineering Research Center, University of California, Berkeley.

Cornell, C.A., and Krawinkler, H., (2000), "Progress and Challenges in Seismic Performance Assessment," *PEER Center News*, Vol 3, No. 2.

Ketchum, M., Chang, V. and Shantz T., (2004), "Influence of Design Ground Motion Level on Highway Bridge Cost," PEER Lifelines Project Number 6D01 Report, Pacific Earthquake Engineering Research Center, University of California, Berkeley.

Mackie, K.R., and Stojadinovic, B., (2006), "Fourway: a Graphical Tool for Performance-based Earthquake Engineering, " *J. Struct. Engineering*, Vol. 132, No. 8, pp. 1274-1283.

Mackie, K., Wong, J-M., and Stojadinovic, B., (2006), "Method for Post-earthquake Highway Bridge Repair Cost Estimation," presented at the *5th National Seismic Conference on Bridges and Highways*, September 18-20, 2006.

Mackie, K.R., and Stojadinovic, B., (2007), "R-factor Parameterized Bridge Damage Fragility Curves," *J. Bridge Engineering*, Vol. 12, No. 4, pp. 500-510.

Mackie, K., Wong, J-M., and Stojadinovic, B., (2007), "Comparison of Post-earthquake Highway Bridge Repair Costs," presented at the *ASCE Structures Congress*, May 16-19, 2007.

Mackie, K., Wong, J-M., and Stojadinovic, B., (2008), "Integrated Probabilistic Performance-based Evaluation of Benchmark Reinforced Concrete Bridges," Report No. 2007/09, Pacific Earthquake Engineering Research Center, University of California, Berkeley.

Wong, J-M., Mackie, K., Porter, R., and Stojadinovic, B., (2008), "Reinforced Concrete Bridge Seismic Damage and Loss Scenarios," to appear at the *6th National Seismic Conference on Bridges and Highways*, July 27-30, 2008.